Forecasting Seasonal Influenza in the United States Using Nonlinear Time Series Analysis

Alicia Kraay,[1*]Rachel E. Gicquelais,[1*] Ramona Roller,[†]Kyle Lemoi,[‡]
Elaine M. Bochniewicz,[‡] Spencer J. Fox[§]

[1]Authors contributed equally

November 2017

Abstract

Forecasting of seasonal infectious diseases, such as influenza, can help in public health planning and outbreak response. We compared a traditional influenza forecasting method (an autoregressive moving average [ARMA] model) with a nearest neighbor forecasting approach (the Lorenz Method of Analogues), where nearest neighbors were identified from the delay reconstructed state space. Delay reconstruction and ARMA models used influenza-like-illness (ILI) surveillance data from 1997-2017 in the United States. We compared model forecasts of the 2015-2017 influenza seasons across 1-4 week prediction horizons. Overall, ARMA models more accurately predicted ILI than the method of analogues, especially when the prediction horizon was 1-2 weeks. The method of analogues with a single nearest neighbor predicted slightly better than the ARMA model for 3-4 weeks; however, a very large delay vector was required. Future directions will include exploring other methods to incorporate nearest neighbors into the method of analogues and combining both autoregressive and nearest neighbor approaches.

1 Introduction

Infectious diseases are a major cause of morbidity and mortality worldwide. Many infectious disease have known pathologies, treatments, and vaccines, but their intrinsic dynamics make it difficult for public health officials to properly

*University of Michigan
†University of Amsterdam
‡MITRE Corporation
§University of Texas at Austin

prepare for inevitable epidemics. If public health officials could accurately predict where and when epidemics would take off, they could allocate resources and implement preventative measures to mitigate morbidity and mortality, or save resources in epidemic situations expected to diminish on their own. For this reason, many organizations have recently sponsored forecasting challenges to compare forecasting methods and spark innovation. The CDC has sponsored the Flu challenge, the NIH with Ebola, and NOAA with Dengue [27, 1, 19]. A wide array of forecasting models have been used in these prediction challenges, but the most accurate models tend to be highly specific, fine-tuned mathematical models describing the transmission dynamics of a disease. Translating the success of these models to other disease prediction necessitates developing and fine-tuning a completely new model.

The optimal method of forecasting infectious disease dynamics depends on the prediction time horizon; mechanistic approaches provide the most accurate predictions over long time horizons. Many forecasts attempt only to supplement traditional epidemiological data with digital data to predict current epidemic status [6, 9, 18]. So called "nowcasts" supplement epidemiologic surveillance data with digital data while surveillance data are compiled, a process which takes about two weeks for traditional influenza surveillance in the United States [16]. Forecasts with longer prediction horizons often necessitate statistical or mechanistic models to account for the infectious process by which current cases give rise to future cases. A major advantage of mechanistic models is their incorporation of explicit epidemiological processes to constrain forecasts. Statistical methods benefit from their generalizability, yet require distributional and independence assumptions that challenge their application to forecasting.

Epidemics are known to exhibit complex and chaotic behavior, and the case data used to understand these dynamics are noisy and biased [23, 2]. Forecasting methods therefore must manage issues related to both nonlinear dynamics and statistical inference. Recent advances in forecasting have often focused on the latter, and have developed complex statistical filtering and ensemble averaging methods that have improved epidemiologic parameter estimation [28]. However, traditional methods for nonlinear time series analysis have rarely been applied to disease dynamics, and present a flexible framework that could be broadly applicable for disease prediction. So far, they have been useful for understanding the relationship between Lyapunov exponents and epidemiological $\mathcal{R}_0$, which is the expected number of secondary cases from a single infectious individual in a fully susceptible population and is a threshold for epidemic emergence ($\mathcal{R}_0 > 1$). Nonlinear time series analysis has been shown to successfully forecast measles dynamics but has not yet been applied to other infectious diseases surveilled in the United States [23]. However, nonlinear time series analysis has been shown to assist forecasts of many biological systems without necessitating a mechanistic model [5, 4, 23].

Here we use a nonlinear time series analysis method that transforms raw disease time series data into a reconstructed state space through delay coordinate embedding, a process that can elucidate the underlying generative process without necessitating a mechanistic model [4, 20, 24, 21]. Using the transformed

dataset, we then forecast seasonal epidemic dynamics for influenza using the method of analogues [17, 26]. We compare these forecast results to a traditionally used forecasting method, an autoregressive moving average model [3]. We compared the performance of the two methods using the Mean Absolute Scaled Error (MASE) [14]. Results from the delay coordinate embedding-based method to date do not improve forecasting beyond the autoregressive model. However, several additional steps may improve the ability of forecasting from the delay reconstructed space to forecast influenza, and these are discussed in the future directions.

2 Methods

2.1 United States (US) Influenza Surveillance Data

Influenza data were extracted from the World Health Organization website for all US flu seasons from 1997 to the present. We used the weighted prevalence of influenza like illness (ILI) to fit our models. For the first four seasons of data collection, surveillance data were missing during the summer months. As flu maintains only low levels of prevalence during these months, we used linear interpolation to fill in the missing summer data prior to using it for forecasting. In total, we used 1,047 weeks of reported flu prevalence for forecasting, with 95 interpolated weeks.

2.2 Traditional Time Series Analysis: Autoregressive Model

We first forecasted influenza using an autoregressive model [3]. We optimized fit of a seasonal autoregressive integrated moving average (SARIMA) model to the influenza data with 1-4 weeks lag using the 'auto.arima' from the 'forecast' package in R [3, 13]. To do so, we wrote a loop and passed all data to the forecast function up to time t and then forecasted a specified number of weeks ahead (h, where h ranges from 1 to 4 as described below). We trained this traditional time series model using 90% of the data to select the optimal S, P, D, and Q parameters as well as to evaluate if there was any evidence for a seasonal component. We then re-fit the model parameters assuming the fixed structure to forecast 1, 2, 3, and 4 weeks ahead. We also calculated the 95% prediction intervals for each forecast.

2.3 Reconstructing the State Space Using Delay Coordinate Embedding

Delay coordinate embedding (DCE) is a method to reconstruct a delay vector from the original time series and requires selection of two embedding parameters, m and τ. This delay vector depends on the embedding dimension m and the delay τ. The parameter m describes the number of dimensions (i.e., observations) needed to reconstruct the signal and τ refers to the spacing between these dimensions, and can be thought of as a lag parameter.

Based on the parameters, a delay vector can be constructed as below.

$$x = [x(t), x(t-2\tau), x(t-3\tau), \ldots, x(t-(m-1)*\tau)]$$

Conceptually, the delay vector reconstruction can be thought of as a comb with prongs sliding over the dataset. The number of prongs refers to m while τ is the number of values between the prongs. The values in the delay vector are the values hit by the prongs. As a rule of thumb, m should be no smaller than 3^m data points, and ideally one should have 10^m data points [22, 25, 7].

The purpose of state space reconstruction guides the method for selecting the embedding parameters. To meet our primary objective of forecasting, we selected the embedding parameters using a method developed by Garland, James, and Bradley, which maximizes time delayed active information storage to optimize forecasting [8]. In a secondary analysis, we reconstructed the state space using the time delayed mutual information to selected the embedding parameters [10, 12]). The motivation behind this secondary analysis was to examine the topology of the state space and calculate the Lyapunov exponents, which can provide evidence that a system is chaotic [4]. Each of these methods are discussed in detail below.

2.3.1 Optimizing Delay Coordinate Embedding Parameters for Forecasting

To construct the delay vector, we jointly selected the embedding parameters, m and τ, that maximized the time delayed active information storage in the reconstructed space using a method developed by Garland, James, and Bradley (2016) [8]. Adapted from Garland, James, and Bradley, Figure 1 presents a conceptual schematic of the meaning of time delayed active information, whereby information from the past and present are evaluated for their ability to provide information about the future.

To select these values, we first calculated the value of A_τ that maximized the time delayed active information storage in the data using the Kraskov-Stügbauer-Grassberger (KSG) estimator. The optimal m and τ values are selected based on the model that has the highest value of A_τ. The KSG estimator is implemented with a Java package, the Java information dynamics toolkit. Figure 2 describes the full procedure.

2.3.2 Topological Examination: Using Time-Delayed Mutual Information for DCE and Calculation of Lyapunov Exponents

In a secondary analysis aimed to examine the influenza system's topology for evidence of chaotic behavior, we used the time delayed mutual information to select the embedding parameters. The TISEAN *mutual.exe* file, version 3.0.1, was used to estimate the time delayed mutual information of the data (i.e. how much two data points are dependent upon each other [10, 12]).

We also calculated the Lyapunov exponents and plotted phase diagrams to determine if the system was chaotic or contained a chaotic attractor. The

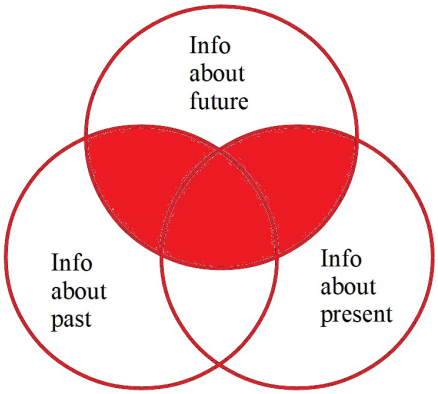

Figure 1: Schematic diagram of time delayed active information (A_τ) adapted from [8]. The time delayed active information quantifies shared information of the past, present, and future. Maximizing this quantity guides selection of DCE parameters optimal for forecasting. In practice, DCE parameter selection is carried out by calculating the value of A_τ that maximizes the time delayed active information storage in the data using the Kraskov-Stügbauer-Grassberger (KSG) estimator.

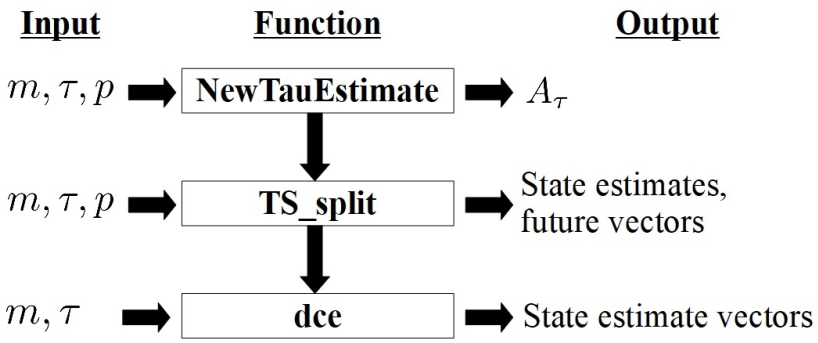

Figure 2: Diagram of procedure for estimating embedding dimensions. In this procedure, the 'NewTauEstimate' function calculates the value of A_τ, the 'TS split' function compiles future (col 1) and current state (cols 2:m) estimates based on the m and τ values, and the delay coordinate embedding ('dce') function partitions the dataset into a matrix of dimensions $[len(timeseries) - \tau, m]$. Each row presents the current state estimate vector based on m (the number of columns) and τ (the time difference or number of observations between column values).

TISEAN Nonlinear Time Series Analysis data package provided Lyapunov exponent estimates using three scripts, *mutual.exe*, $falsenearest.exe$ and *lyapk.exe*, which each output a plain text file with a set of results. The methods must be run in a specific order for successful selection of parameter values. By default, the TISEAN scripts try a variety of values for the parameters. The user must determine the ideal set of values to feed into the final script, *lyapk.exe*, to achieve acceptable results. To interpret each parameter set and visualize results, we wrote custom Python code, which is summarized below in the results section.

2.4 Forecasting Influenza Using the Method of Analogues from the Reconstructed State Space

After selecting the optimal embedding parameters for forecasting as described above, we used the delay reconstructed state space to forecast influenza using the method of analogues [17]. The general idea of the method of analogues is that the future state of the data can be predicted by finding similar observations (i.e. 'analogues') in the observed time series. There are various methods of selecting analogues for forecasting but in this paper, we used a single nearest neighbor method. Briefly, we looked for the nearest neighbour of x(t=n) within all past values in the time series, i.e. the value that is most similar to x(t=n), and used the value that is one step ahead in the future of the nearest neighbour as the prediction for x(t=n).

After selecting the nearest neighbor for the values in our embedded time series, we divided the data into test and training data to conduct the forecasts. We selected the final 103 data points to be forecasted to correspond to the data points predicted by the autoregressive model. To avoid inflating our prediction error, we re-observed the real time series data during our fitting. For the prediction data, we predicted p time steps into the future and added these predicted values to the time series. Without re-observation, nearest neighbor candidates could have included forecasted values, which are less accurate than real data, and as such, would have inflated the overall prediction error. To avoid this issue, we re-observed the system at the $p + 1$ predicted value. That is, rather than predicting the $p+1$ value, we replaced it with the real value of the system at this time point. In this way, our time series still incorporates real values, improving prediction performance. An example for a prediction horizon of three is shown in figure 3.

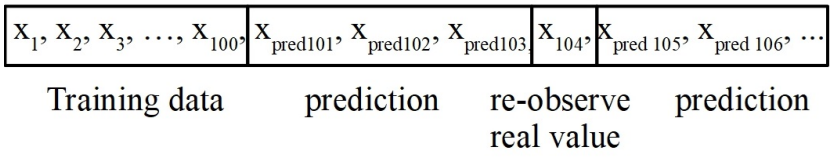

Figure 3: Re-observation of the data during forecasting to improve prediction accuracy.

3 Results

3.1 Traditional Time Series Analysis: Autoregressive Model

The optimal fitted model structure for the influenza surveillance data was an ARIMA(4,0,4) model, which is equivalent to an autoregressive moving average model (ARMA(4,4)). The seasonality and differencing components were found to be insignificant. Forecasts were reasonably good for 1-2 weeks ahead but worsened at 3-4 weeks prediction horizon. Prediction errors were largest during the peaks of the influenza outbreak. Additional details of the ARMA model's fit to data is shown below, following a discussion of the nonlinear time series analysis approach.

3.2 Selection of Parameters for Forecasting from the Reconstructed Space

Choosing m and τ jointly suggested that for short prediction horizons of 1-2 weeks, $m = 2$ and $\tau = 6$ or 5, respectively [7, 8]. For longer prediction horizons of 3-4 weeks, larger values of m=6 and τ=51 weeks were optimal (figure 4). Prediction horizons beyond 4 weeks had maximum values of $A(\tau)$ at even larger values of m and τ. Although we chose the maximum $A(\tau)$ estimate, a smaller value of τ and m may give similar results.

3.3 Comparison of Forecasts: Method of Analogues versus ARMA

The delay reconstructed state space was used to forecast the final 103 points of the 1,030 data points in the ILI dataset using the method of analogues for four prediction horizons (1-4 weeks) with the maximum $A(\tau)$ value (m and τ parameters with most shared information about the future). We used the simplest version of the method of analogues: forecasting from a single nearest neighbor.

Forecasting results are summarized below by fit to data, alongside the ARMA model described above (figure 5). The Mean Absolute Scaled Error (MASE), a summary statistic of each forecast's fit to ILI data, is presented in table 1 [14]. A MASE < 1 indicates a superior fit of the forecasts to data. In contrast, a MASE$>$1 indicates that a random walk model, where the previous time period's data point is used as the forecast, would be superior to either method.

The ARMA model generally outperformed the method of analogues with 1 nearest neighbor, as indicated by superior fit to data and lower MASE values, especially for 1 and 2 week ahead forecasts. The optimal delay (τ) for 3 and 4 week predictions was 51, representing a delay of nearly 51 weeks, or one year prior, to be used in the state space reconstructions and candidates for nearest neighbors. Under these conditions, the method of analogues outperformed the ARMA model, but these results should be interpreted with caution given the large parameter values.

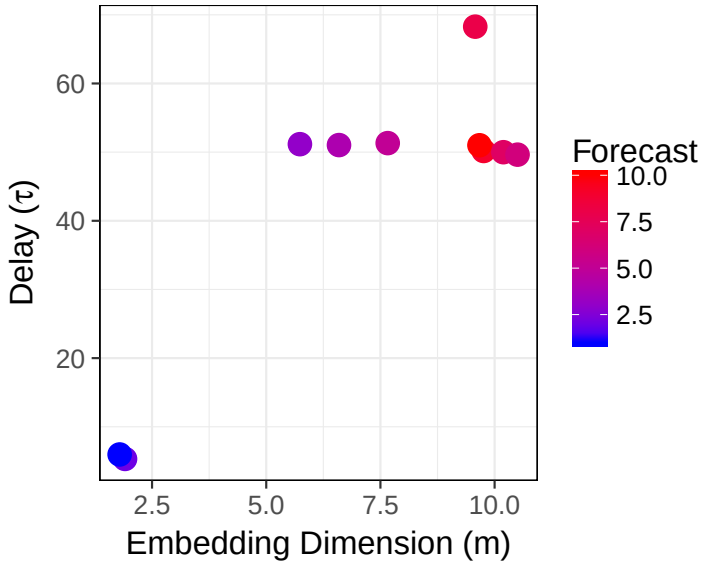

Figure 4: Optimal Delay Coordinate Embedding Parameters for Forecasting. Values for m and τ were selected by maximizing the value of A_τ, the time delayed active information storage in the data, using the Kraskov-Stügbauer-Grassberger (KSG) estimator, at forecast horizons of 1-10 weeks ahead. Longer delays and higher embedding dimensions were required beyond forecasting horizons of two weeks.

Forecasting Method	Weeks Ahead	MASE
Method of Analogues with Delayed Coordinate Embedding	1	1.757
	2	0.983
	3	0.924
	4	0.720
Autoregressive Moving Average (ARMA) Model	1	0.602
	2	0.810
	3	0.978
	4	1.125

Table 1: Comparison of model performance by prediction horizon.

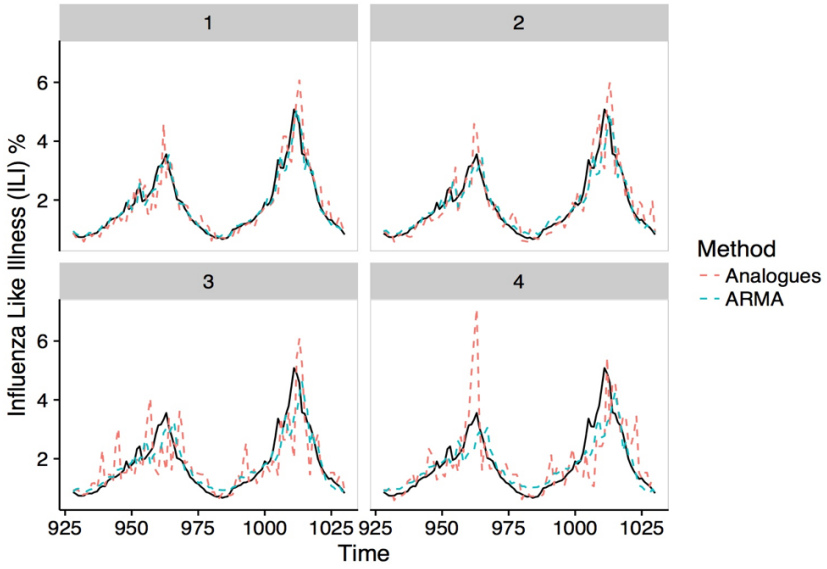

Figure 5: Fit to ILI data by ARMA versus method of analogues with DCE. Forecasted points from an ARMA model (green) and the method of analogues forecasts using one nearest neighbor identified from the DCE state space reconstruction (salmon) are shown in comparison to the observed ILI data (black).

3.4 Topological Examination to Determine Lyapunov Exponents

We used results from the *mutual.exe* and $falsenearest.exe$ methods to choose $\tau = 15$ as the delay for topological reconstruction from the ILI surveillance data. The *lyapk.exe* function was next run with a minimal dimension of 2 and a maximal dimension of 6. These results supported that ILI data were ill-suited for calculating the Lyapunov exponent. Viewing the plots of the Lyapunov stretching factor, we found no plots with a linear section that could be used to calculate the exponent figure 6. Similar to the simulated SEIR data, the phase diagrams with τ and a 2 * phase shifts implied that the ILI data are periodic and not chaotic.

4 Discussion

In this analysis, we successfully used delay coordinate embedding to forecast seasonal influenza. While the simplest version of this method did not outperform an autoregressive moving average model, more detailed methods that can harness the full power of the DCE and method of analogues approach may hold more promise. Ultimately, the method of analogues may be particularly useful for longer prediction horizons. For many infectious diseases, case reporting can

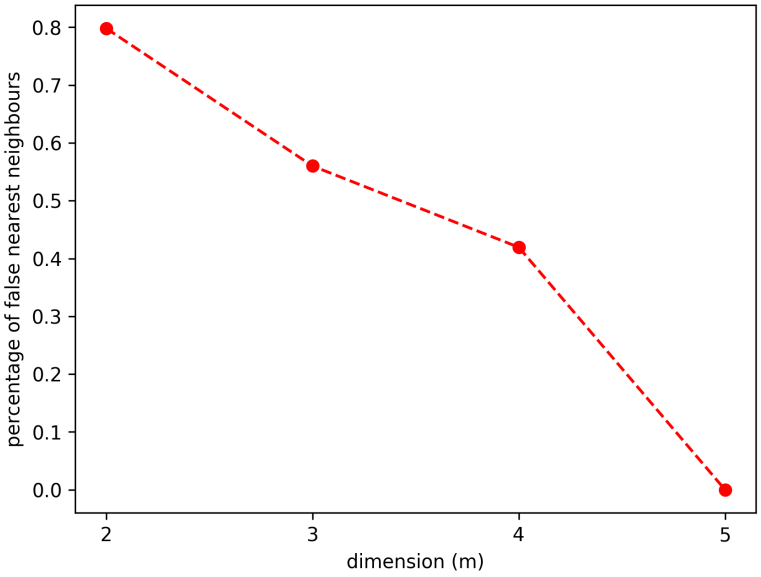

Figure 6: Graphical representation of the false nearest neighbor TISEAN script output ($falsenearest.exe$) for determining the Lyapunov exponent from the influenza surveillance data. From this graph, we determined the embedding dimension, m, which is used as part of the formula to find the Lyapunov Exponent.

be delayed for several weeks and forecasts are needed to fill this gap [16, 6, 9, 18].

We used the simplest possible method of analogues in this analysis by relying on only one nearest neighbor. More complex methods that take advantage of information in other locations of the time series are likely to produce even better results [26, 29]. Our results suggest that using delay coordinate embedding and the method of analogues to forecast infectious disease dynamics may be promising and we will explore its use further in future research.

For both methods, the predictions were less accurate with longer forecasting horizons. However, the method of analogues performed better than a simpler ARMA model for longer prediction horizons, as indicated by its lower mean absolute scaled error (MASE). This result suggests that combining information from ARMA and analog prediction methods might produce better forecasts than either method alone. More work is needed to develop hybrid methods that can leverage the advantages of each. In addition, comparison of either approach to the prediction accuracy of mechanistic models (e.g. susceptible-exposed-infected-recovered [SEIR]) commonly used in forecasting influenza is required.

Although not discussed here, we also attempted to forecast seasonal dynamics from a simulated SEIR model. While the results were not promising and therefore not shown in this report, we learned several lessons that may guide future directions for influenza forecasting. The difficulty with forecasting the simulated SEIR data most likely resulted from adding too much noise to preserve the underlying structure. This result suggests that this particular method is highly sensitive to measurement error, even when such error is random. In general, disease surveillance data are unlikely to overestimate the current infection burden and are much more likely to underestimate it. In other forecasting methods, this measurement uncertainty is often accounted for explicitly [15, 11]. However, in our analyses of both the influenza and SEIR data, we did not explicitly account for the reporting rate or its distribution. It is possible that this method could perform better when measurement error is either non-random or is explicitly accounted for in the model fitting. Follow-up analyses could assess the sensitivity of our forecasting methods to different types of error structures.

Future work forecasting other seasonal diseases would be useful and could provide a conceptual framework for identifying which diseases the delay coordinate embedding method could help forecast. In addition, these comparisons may help identify important differences in epidemic dynamics for diseases that appear, on the surface, to exhibit similar seasonality.

4.1 Next Steps: Influenza Like Illness Forecasting

Our group plans to pursue several additional analyses to improve our existing ILI forecasts to better match empirical influenza data and provide more rigorous comparisons to existing influenza forecasting methods. First, we will apply additional state space reconstruction methods, such as multiview embedding, which may improve our ability to forecast from the relatively short ILI time series available [30]. Next, we will optimize our neighbor searching algorithm for

time series forecasting by comparing several approaches. Similar to an approach used by Viboud et al. [26], we will forecast points by weighting the values of >1 nearest neighbors in the delay reconstructed space. In addition, we will weight nearest neighbors based on characteristics of circulating seasonal viruses, such as genetic distance between the forecasted season's circulating strain and strains from prior seasons. This approach would weight similar strains more heavily than more genetically distant strains. We will also apply more sophisticated nearest neighbor approaches, such as the simplex method [29]. To identify promising candidates for accurate influenza forecasting, all methods will be compared using the mean absolute scaled error.

Once we have identified an optimal strategy to reconstruct the state space and identify nearest neighbors for forecasting, we will compare our optimized results to the method of analogues approach without delay coordinate embedding. This analysis will illustrate the advantages and/or drawbacks of applying state space reconstruction and allow for a direct comparison of our results to an existing analysis using the method of analogues by Viboud et al. [26]. Our overarching goal in pursuing these next steps is to identify optimal strategies for forecasting short- (1-2 weeks ahead) and long-term (seasonal) prediction horizons.

4.2 Conclusion

Forecasting influenza using the method of analogues from a state space reconstruction obtained via delay coordinate embedding may complement existing methods to forecast seasonal influenza. Further work to compare and combine this method with existing forecasting methods, such as autoregressive models, will determine the feasibility and utility of incorporating this approach into existing influenza forecasting efforts.

4.3 Acknowledgments

The authors thank Dr. Joshua Garland for his contributions to this work. In addition, the authors thank the Santa Fe Institute's 2017 Complex Systems Summer School for their support of this work.

References

[1] Matthew Biggerstaff, David Alper, Mark Dredze, Spencer Fox, Isaac Chun-Hai Fung, Kyle S Hickmann, Bryan Lewis, Roni Rosenfeld, Jeffrey Shaman, Ming-Hsiang Tsou, Paola Velardi, Alessandro Vespignani, and Lyn Finelli. Results from the centers for disease control and prevention's predict the 2013–2014 Influenza Season Challenge. *BMC Infectious Diseases*, 16(1):1–10, 2016.

[2] Benjamin Bolker and B T Grenfell. Chaos and biological complexity in

measles dynamics. *Proceedings. Biological sciences / The Royal Society*, 251(1330):75–81, jan 1993.

[3] George EP Box and Gwilym M Jenkins. *Time series analysis: forecasting and control, revised ed.* Holden-Day, 1976.

[4] Elizabeth Bradley and Holger Kantz. Nonlinear time-series analysis revisited. *Chaos*, 25(9), 2015.

[5] Ethan R Deyle, M Cyrus Maher, Ryan D Hernandez, Sanjay Basu, and George Sugihara. Global environmental drivers of influenza. *Proceedings of the National Academy of Sciences of the United States of America*, page 201607747, 2016.

[6] C P Farrington, N J Andrews, A D Beale, and M A Catchpole. A statistical algorithm for the early detection of outbreaks of infectious disease. *J R Stat Soci Ser A (Stat Soci)*, 159:547–563, 1996.

[7] Joshua Garland and Elizabeth Bradley. Prediction in projection. *Chaos: An Interdisciplinary Journal of Nonlinear Science*, 25(12):123108, 2015.

[8] Joshua Garland, Ryan G. James, and Elizabeth Bradley. Leveraging information storage to select forecast-optimal parameters for delay-coordinate reconstructions. *Phys. Rev. E*, 93:022221, Feb 2016.

[9] T Garske, J Legrand, C A Donnelly, H Ward, S Cauchemez, C Fraser, and et al. Assessing the severity of the novel influenza a/h1n1 pandemic. *British Medical Journal*, 339, 2009.

[10] Kantz H. and Schreiber T. *Nonlinear Time Series Analysis, 2nd Edition.* Cambridge University Press, 2004.

[11] Daihai He, Edward L Ionides, and Aaron A King. Plug-and-play inference for disease dynamics: measles in large and small populations as a case study. *Journal of the Royal Society Interface*, 7, 2010.

[12] Kantz H. Hegger R. and Schreiber T. Practical implementation of nonlinear time series methods: The TISEAN package. *Chaos*, 9, 1999.

[13] R J Hyndman. *forecast: Forecasting functions for time series and linear models*, 2017. R package version 8.1.

[14] Rob J Hyndman and Anne B. Koehler. Another look at measures of forecast accuracy. *International Journal of Forecasting*, 22(4):679–688, 2006.

[15] Edward L Ionides, C Bretó, and Aaron A King. Inference for nonlinear dynamical systems. *Procedings of the National Academy of Sciences*, 103:18438–18443, 2006.

[16] Ruth Ann Jajosky and Samuel L Groseclose. Evaluation of reporting timeliness of public health surveillance systems for infectious diseases. *BMC Public Health*, 4, 2004.

[17] Edward N Lorenz. Atmospheric predictability as revealed by naturally occurring analogues. *Journal of the Atmospheric sciences*, 26(4):636–646, 1969.

[18] A Nicoll, A Ammon, Gauci A Amato, A Amato, B Ciancio, P Zucs, and et al. Experience and lessons from surveillance and studies of the 2009 pandemic in europe. *Public Health*, 124:14–23, 2010.

[19] NOAA. Dengue Forecasting. 2016.

[20] Norman H Packard, James P Crutchfield, J Doyne Farmer, and Robert S Shaw. Geometry from a time series. *Physical review letters*, 45(9):712, 1980.

[21] Tim Sauer, James A Yorke, and Martin Casdagli. Embedology. *Journal of statistical Physics*, 65(3):579–616, 1991.

[22] Leonard A Smith. Intrinsic limits on dimension calculations. *Physics Letters A*, 133(6):283–288, 1988.

[23] George Sugihara and Robert M. May. Nonlinear forecasting as a way of distinguishing chaos from measurement error in time series, 1990.

[24] Floris Takens et al. Detecting strange attractors in turbulence. *Lecture notes in mathematics*, 898(1):366–381, 1981.

[25] AA Tsonis, JB Elsner, and KP Georgakakos. Estimating the dimension of weather and climate attractors: important issues about the procedure and interpretation. *Journal of the atmospheric sciences*, 50(15):2549–2555, 1993.

[26] Cécile Viboud, Pierre-Yves Böelle, Fabrice Carrat, Alain-Jacques Valleron, and Antoine Flahault. Prediction of the spread of influenza epidemics by the method of analogues. *American Journal of Epidemiology*, 158:996–1006, 2003.

[27] Cécile Viboud, Kaiyuan Sun, Robert Gaffey, Marco Ajelli, Laura Fumanelli, Stefano Merler, Qian Zhang, Gerardo Chowell, Lone Simonsen, and Alessandro Vespignani. The RAPIDD Ebola Forecasting Challenge: Synthesis and Lessons Learnt. *Epidemics*, (April), 2017.

[28] Wan Yang, Alicia Karspeck, and Jeffrey Shaman. Comparison of filtering methods for the modeling and retrospective forecasting of influenza epidemics. *PLoS computational biology*, 10(4):e1003583, apr 2014.

[29] Hao Ye, Richard J Beamish, Sarah M. Glaser, Sue C. H. Grant, Chih-hao Hsieh, Laura J. Richards, J T Schnute, and George Sugihara. Equation-free mechanistic ecosystem forecasting using empirical dynamic modeling. *Procedings of the National Academy of Sciences*, 112:E1569–E1576, 2015.

[30] Hao Ye and George Sugihara. Information leverage in interconnected ecosystems: Overcoming the curse of dimensionality. *Science*, 353(6302):922–925, 2016.